HgTe/HgCdTe Superlattices Grown on CdTe/Si by Molecular Beam Epitaxy for Infrared Detection

Y. SELAMET,[1,3] Y.D. ZHOU,[1] J. ZHAO,[1] Y. CHANG,[1] C.R. BECKER,[2] R. ASHOKAN,[1] C.H. GREIN,[1] and S. SIVANANTHAN[1]

1.—Microphysics Laboratory, University of Illinois at Chicago, Chicago, IL 60637. 2.—Physikalisches Institut der Universitat Wurzburg, A M Hubland 97074 Wurzburg, Germany. 3.—E-mail: yselam1@uic.edu

High-quality HgTe/CdTe superlattices (SLs) and device structures incorporating them were grown by molecular beam epitaxy (MBE) on CdTe/Si substrates. In-situ techniques, such as reflection, high-energy electron diffraction and spectroscopic ellipsometry, were extensively used to rigorously control the growth parameters. The full width at half maximum (FWHM) of x-ray double-crystal rocking curves (DCRCs) were 100–150 arcsec, comparable to those of HgCdTe alloys grown on the same type of substrates. The room-temperature Fourier transform infrared (FTIR) spectrum exhibits two-dimensional features characteristic of SLs. Trial devices in a p^+-n^--n^+ format were fabricated by diffusing gold in order to further evaluate the HgTe/CdTe SL performance. Gold diffusion was chosen to fabricate photovoltaic junctions in order to preserve the structural integrity of the SLs during the device processing. Though no attempt was made in the current study to optimize the junction properties by Au diffusion, this method has proven to be very useful for rapid preliminary evaluation. The measured spectral-response and detectivity data indicate the possibility to fabricate photovoltaic devices on an HgTe/CdTe SL, although further work is needed to optimize the p-n junction fabrication.

Key words: CdTe/Si substrates, x-ray, rocking curves, superlattices, MBE

INTRODUCTION

An infrared (IR) photon detector operating at temperatures higher than the current ones will eliminate the expensive cryogenic-cooling equipment, improve the reliability of imaging systems, and greatly improve the yield. To achieve background limited performance (BLIP), the cooling requirements of current IR detectors depend on the cutoff wavelength. Theoretically, the detectors need to be cooled to about 180 K to 20 K for cutoff wavelengths varying from the mid-wavelength infrared (MWIR) to very long wavelength infrared (VLWIR) region, respectively. Increasing the BLIP operation temperature of these detectors, especially in the long wavelength region, is highly desirable and critical for various space applications.

Increasing minority carrier-recombination lifetimes would lead to higher operating temperatures without performance degradation. There are two intrinsic carrier-recombination mechanisms: Auger and radiative. The third limiting mechanism, Shockley–Read–Hall recombination, is due to defects and impurities in the sample that give rise to trap levels in the energy gap. The effects of this limiting mechanism can be reduced by optimizing growth conditions and/or post-growth thermal treatment. The Auger recombination rate strongly depends on the carrier concentration (increases as the square of the carrier concentration at low and moderate concentrations and at a slower rate at higher concentrations when carriers are degenerate). The radiative recombination rate, on the other hand, increases only linearly with the carrier concentration and is not the limiting mechanism throughout most of the operating temperature region for long wavelength detectors.

In the VLWIR region, extrinsic materials, such as doped Si and Ge with impurity band conduction, are typically used as IR detectors. However, these

(Received October 16, 2003; accepted January 21, 2004)

materials have millimeter-scale absorption lengths and cannot be used to form large area arrays. Also, these detectors operate at very low temperatures (20 K or below), limiting their applications. Intrinsic detectors have several inherent advantages over extrinsic detectors. They have higher quantum efficiencies, absorption coefficients, and operating temperatures, leading to large format arrays. However, achieving VLWIR cutoff control with intrinsic alloy materials is very difficult. At these wavelengths, HgCdTe has a very narrow bandgap, and any small variation in the Cd mole fraction translates into a large variation in the cutoff wavelength. The HgTe/CdTe superlattices (SLs) are relatively more robust against composition variations because the cutoff wavelength is controlled by the well thicknesses. Layer thickness can be controlled down to atomic scales with molecular beam epitaxy (MBE) growth.

The HgTe/CdTe SLs have additional advantages including a near lattice match (~0.3% mismatch) between HgTe and CdTe and a common anion, Te. The HgTe/CdTe SLs can be more stable than HgCdTe alloys because of a spatial separation of HgTe and CdTe layers.[1]

The HgTe/CdTe SL-based IR photovoltaic detectors are expected to have lower tunneling currents because of a larger effective mass in the growth direction, which is inversely related to the CdTe barrier width, d_b. For a large d_b, the perpendicular effective mass is also large and tunneling current low, whereas the opposite is true when d_b is small. However, if the effective mass is too large, then perpendicular transport is no longer possible. Therefore, a compromise is required to achieve a reduced tunneling current with a sufficiently large vertical transport. This requires the perpendicular effective mass to be about ten times larger than the in-plane effective mass and $d_b \approx 5$ nm.

This paper describes our preliminary studies on the growth and characterization of HgTe/CdTe SLs with cutoff wavelength in the MWIR region. Diffusion of Au was employed here as a quick method to evaluate the possibility of photovoltaic p-n junction fabrication while ensuring low process temperatures during the device fabrication in order to prevent interdiffusion of the SL layers. Further rigorous work is required to optimize the photovoltaic junction design and fabrication to exploit the advantages of higher effective masses in the growth direction.

MATERIAL GROWTH AND CHARACTERIZATION

The HgTe/CdTe SLs were grown on CdTe/Si substrates. Both single SL layers and device structures incorporating SLs were studied. Although HgTe/CdTe SL materials have been studied in the past, reports on SL-based structures and devices are very few. An IR detector structure incorporating carrier exclusion (at the bottom n^+ layer/absorber interface) and carrier extraction (at the top p^+ layer/absorber interface) is shown in Fig. 1. The figure shows a top

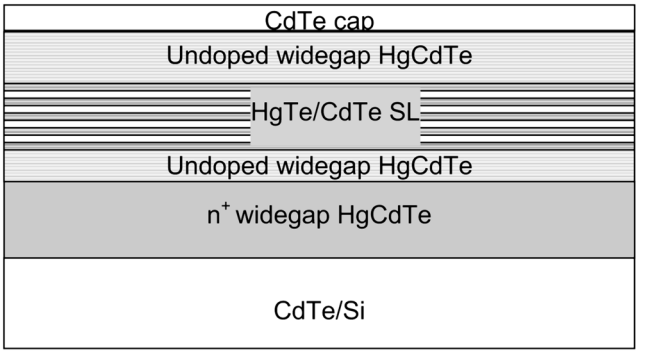

Fig. 1. Layer layout of the as-grown IR detector structure, incorporating a SL as the absorber layer.

undoped layer that is later converted to a p+ region by Au diffusion. The excluding and extracting layers are made of the HgCdTe alloy with Cd mole fractions of x = 0.35–0.4. The layer between the absorber layer (slightly n-type HgTe/CdTe SL) and the bottom excluding n^+ layer is an undoped, widegap HgCdTe buffer to reduce the possibility of a doping tail in the active absorber layer. Attention must also be given to the interface between the SL layer and HgCdTe alloy layers in order to smooth out barriers caused by the energy band discontinuities. The SL growth started with a HgTe layer and ended with another HgTe growth to avoid extra CdTe barriers that hinder carrier transportation. The uppermost CdTe cap layer acts as a device passivant.

Increasing the operating temperature of an IR detector by depleting the carriers in the absorber region through the use of a higher operating temperature (HOT) architecture requires that the absorber layer have a low carrier concentration and be composed of high-quality material. It should be thinner than the diffusion length, yet thick enough for IR absorption. The n^+ and p^+ layers should have a wider bandgap than the absorber layer. Also, the n^+ exclusion layer should be thick enough, at least three times the minority carrier-diffusion length, to inhibit minority carrier injection into the undoped layer from this layer.

Before starting the SL growth, the growth rates of HgTe and CdTe were calibrated using in-situ ellipsometry and ex-situ step profiling. The calibration data were used to control the thicknesses of the HgTe wells and CdTe barriers.

During the SL growth, the Te_2 and CdTe cell shutters were opened sequentially under a fixed Hg flux, which results in HgTe well layers and barrier layers that are close to pure CdTe. According to previously reported results[4] for (211) HgTe/CdTe SLs, the barrier layers are of approximately 90–95% Cd mole fraction.

We closely monitored the reflection, high-energy electron diffraction patterns at the beginning and during the growth. They were all streaky from the start of the bottom n^+ layer and throughout the SL and top undoped layers. We concluded that the temperature stabilization was optimal, and the crystalline quality of the layers was good.

The cell temperatures were controlled to ±0.1°C over the entire growth procedure to ensure stable fluxes. During growth, the steady-state values of the CdTe, Te, and Hg fluxes were selected to give a HgTe/CdTe SL growth rate of about 2–3 Å/sec, which is much lower than the HgCdTe alloy growth rate of 6–8 Å/sec. The lower growth rate provides us with better control over the thickness of HgTe wells and CdTe barriers. The difference in growth rates for the HgTe/CdTe SL and HgCdTe alloy layers leads to different growth conditions. We reduced the CdTe and Te fluxes to lower the growth rate, and, at the same time, the Hg flux was reduced according to the corresponding Te flux necessary to maintain good crystal quality. All these changes were made after completing the bottom HgCdTe alloy growth and were made again after completing the HgTe/CdTe SL before starting the top HgCdTe-alloy growth. The CdTe, Te, and In cell temperatures and Hg fluxes during the structure growth are shown in Fig. 2.

In-situ ellipsometry data was also collected during HgTe/CdTe SL growth and is shown in Fig. 3. It shows a periodic change in the SL optical properties alternating growth of HgTe and CdTe layers. We can observe two superimposed periodicities. The slower oscillation is due to the progressive increase in total thickness. This oscillation dies out once the layer is optically thick. The shorter-period oscillation is due to the successive deposition of materials characterized by different indices of refraction. The period of the shorter oscillation can be used to estimate the growth rate of HgTe layers. The calibration of the CdTe growth rate is not easily done by ellipsometry because it cannot distinguish between the CdTe SL layers and the CdTe in the CdTe/Si substrates. Therefore, we resorted to step profiling. We also checked the results of our ellipsometric growth rates against those obtained with step profiling and obtained good agreement between the two.

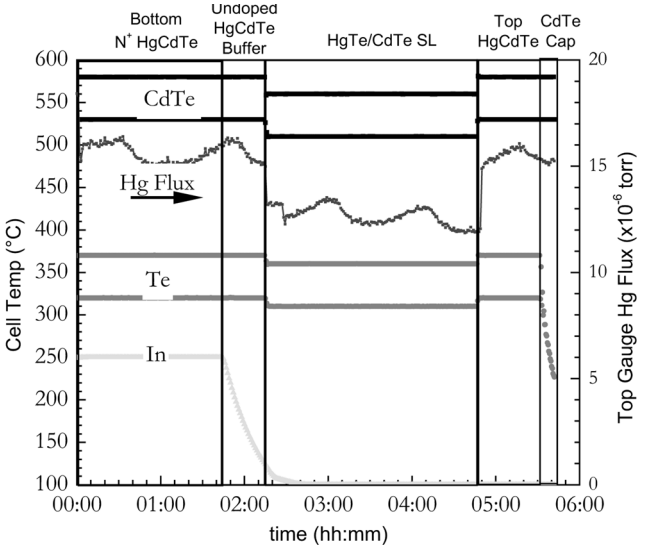

Fig. 2. The CdTe and Te cell temperatures and Hg flux as a function of growth time during growth of one of the device structures by MBE.

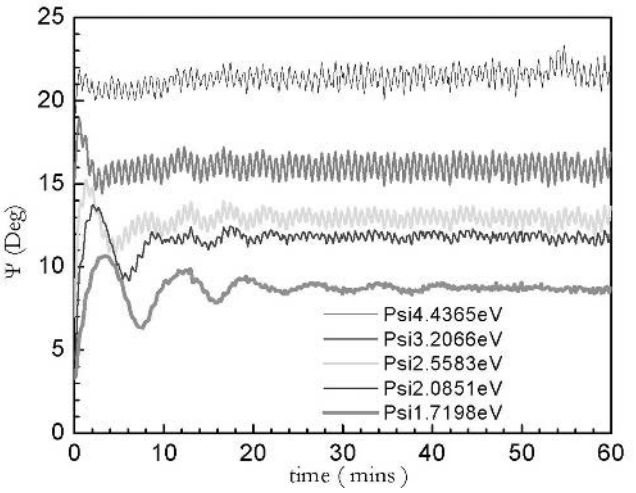

Fig. 3. In-situ ellipsometry data showing periodic changes in the angle of the differential amplitude ratio of the complex Fresnel coefficients of the SL as a function of the growth time caused by the periodic growth of HgTe and CdTe layers.

The crystalline quality of the material was studied using double-crystal rocking curves (DCRCs). Figure 4 shows the DCRCs of the detector structure. X-ray diffraction shows two peaks. Peak 1 located at −657.5 arcsec is less intense and is attributed to the SL because the top HgCdTe alloy layer weakens and broadens the SL diffraction signal. The DCRC full-width at half-maximum (FWHM) for peak 1 is 110 arcsec. Peak 2, located at −8.9 arcsec, is attributed to the HgCdTe-alloy layers. The DCRC FWHM for peak 2 is 122 arcsec, implying good crystal quality. These FWHM values are comparable to those of HgCdTe alloys grown on CdTe/Si substrates.

Experimental Fourier transform infrared (FTIR) spectra show features caused by both HgCdTe-alloy layers and the HgTe/CdTe SL. The representative FTIR spectrum at 295 K of Fig. 5 shows absorption caused by different subband transitions. From the calibration runs, we expect the HgCdTe-alloy cutoff

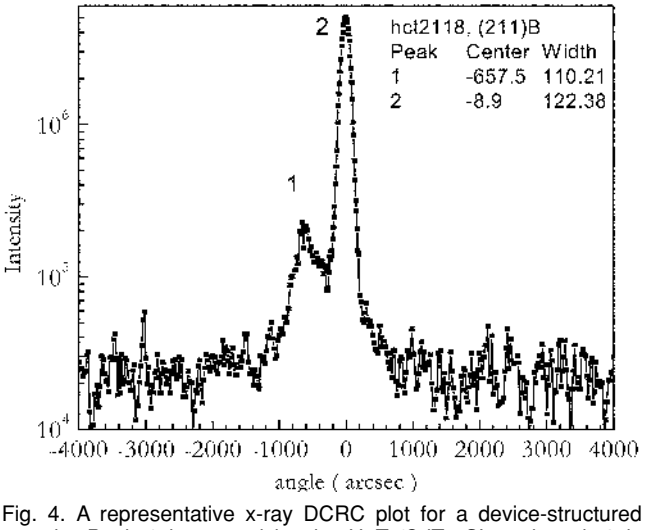

Fig. 4. A representative x-ray DCRC plot for a device-structured sample. Peak 1 is caused by the HgTe/CdTe SL and peak 2 is caused by HgCdTe-alloy layers.

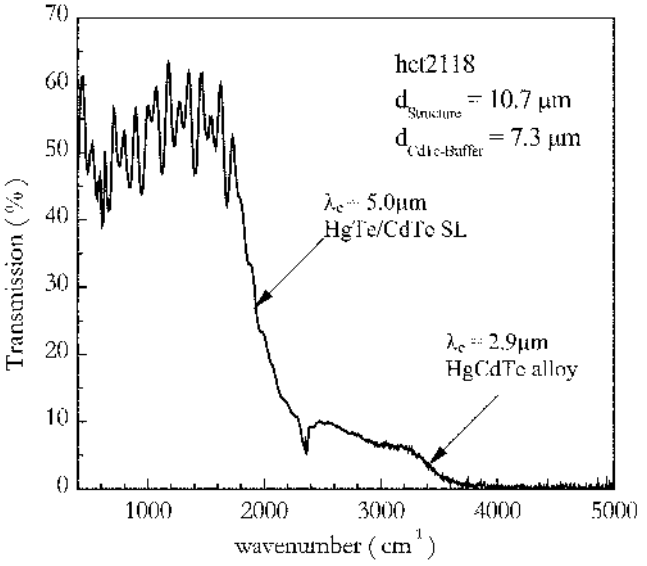

Fig. 5. The FTIR spectra of sample hct2118 at 295 K, showing features of both the HgCdTe alloy and HgTe/CdTe SL.

to be around 3,400 cm^{-1} or 2.94 μm in the wavelength scale because the targeted layer composition was around x = 0.38. This is in good agreement with the experimental feature at about 2.9 μm. The cutoff for the HgTe/CdTe SL is seen to be at 5 μm. The FTIR data of single HgTe/CdTe SL layers (not device structures) display a similar feature near 5 μm. The absorption coefficient has been calculated for an alloy with x = 0.38 and a SL with well and barrier widths of 34 Å and 40 Å, respectively, as shown in Fig. 6. Theoretical details can be found elsewhere.[2] Agreement with experiment is good at 295 K. From the theoretical absorption coefficient for 80 K, the absorption edge of the alloy only shifts from 2.9 μm to 3.05 μm, whereas the absorption edge caused by the SL shifts from about 5 μm to 7 μm, which is in very good agreement with the spectral response discussed later.

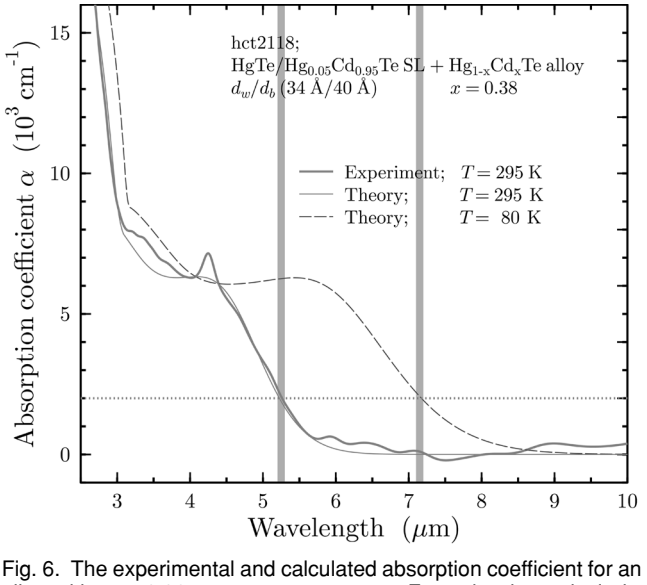

Fig. 6. The experimental and calculated absorption coefficient for an alloy with x = 0.38 at room temperature. From the theoretical absorption coefficient for 80 K, the absorption edge of the alloy only shifts from 2.9 μm to 3.05 μm, whereas the absorption edge caused by the SL shifts from about 5 μm to 7 μm.

The general behavior of the in-plane electrical properties of an HgTe/CdTe SL is the same as for other narrow bandgap semiconductors as demonstrated by Hall measurements. Figure 7 shows in-plane Hall data (carrier concentration and mobility versus temperature) of one of the single SL layers. Other layers have similar results. The Hall measurements were carried out as a function of temperature using the Van der Pauw geometry. As seen in Fig. 7, the carrier concentration in this SL layer is in the low 10^{15} cm^{-3} range, with n-type mobilities exceeding 10^4 cm^2/Vs.

TEST-STRUCTURE DEVICE FABRICATION AND CHARACTERIZATION

A test structure was fabricated by mesa etching using a bromine methanol solution. The conventional method of converting an undoped-HgCdTe top layer to p^+ is by As ion implantation. After implantation, the structure needs to be annealed at high temperatures to activate the As and reduce extensive surface and lattice damage caused by high-energy ion bombardment. Such a high-temperature (425–450°C) activation and annealing procedure may have adverse effects on the SL interface sharpness and the junction location. Our recent study[3] showed that SLs could not withstand high-temperature annealing because of layer interdiffusion. Longer anneal times increase the interdiffusion of the SL layers. A best case scenario involves annealing at temperature below 235°C for short periods of time, which will not be sufficient for As activation. Consequently, doping with As appears impractical, so we used Au for the p-type conversion of the top HgCdTe layer. Windows in the CdTe cap layer were opened photolithographically for selective gold diffusion. A very thin, ultrahigh-purity

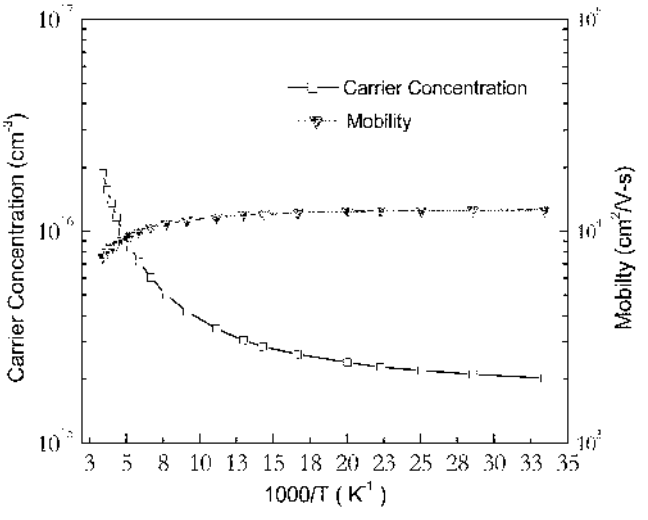

Fig. 7. Hall data of hct2067, a single SL, showing n-type behavior. The sample had nominal HgTe-well and CdTe-barrier thicknesses of 30 Å and 66 Å, respectively. This sample had a cutoff of 5.2 μm at room temperature as measured by FTIR.

Au layer was deposited and sequentially annealed at low temperatures to diffuse the Au into the structure. This method is known to dope samples p-type.[4] However, a systematic study to optimize such junction formation is required to achieve state-of-the-art performance. The primary goal in this study was to form p-n junctions at low enough temperatures to preserve the SL integrity, so that the SL-based detector properties, such as spectral cutoffs, can be evaluated.

The fabricated devices were mounted in a liquid N_2 dewar with a ZnSe window, and spectral-response measurements both at 80 K and room temperature were carried out. Figure 8a and b shows representative spectral-response curves for one of the devices at 80 K and room temperature, respectively. A metal screen was used to reduce the background flux. The device gives a strong signal even at room temperature. In Fig. 8a, two main response peaks are observed. The position of the broader peak at longer wavelength is about 5 μm, which we will refer to as peak 1. The cutoff of this peak is 7 μm. When compared with layers with similar structures and material growth conditions, we conclude that the only possible origin of this signal is the HgTe/HgCdTe SL. Several sub-peaks on this peak may correspond to other intersubband transitions. The position of the other peak (peak 2) is at 2.7 μm, with a cutoff at 3 μm. When compared with the previous layer-growth data, we conclude that it comes from the HgCdTe layers. We also measured the room-temperature spectral response. Assuming peak 2 is due to HgCdTe, we used the Hansen and Schmidt formula[5] to predict the room-temperature positions of the peak and cutoff. The 80-K cutoff of peak 2 gives a predicted value of the room-temperature cutoff at 2.85 μm. From Fig. 8b, we see that these two peaks merge together, and there is a shoulder peak at the position of 2.6 μm with an estimated cutoff at 3 μm, in reasonable agreement with the predicted value. A comparison of the room-temperature spectral-response curve to the room-temperature FTIR data of Figs. 5 and 6 also suggests that this shoulder peak comes from the HgCdTe-alloy layer, and the broader peak to the long wavelength direction (peak 1) comes from the HgTe/HgCdTe SL. Figure 8b shows the position of this broader peak to be at 4.5 μm with a cutoff at 5.4 μm. The room-temperature cutoffs for the HgCdTe alloy and HgTe/CdTe SLs are in good agreement with the ones obtained from room-temperature FTIR measurements. These assignments are corroborated by calculated absorption and transmission spectra.

We also measured detectivities of the test structures. A device with a cutoff at 7 μm results in a specific detectivity of 1.6×10^{10} cmHz$^{1/2}$/W. The corresponding BLIP D* value for a 295-K background and 2π field of view (FOV) is[6] 8×10^{10} cmHz$^{1/2}$/W for photovoltaic devices with this cutoff.

We did not observe any indication of saturation from the detector signal, which would be easily observed in the FTIR results.

CONCLUSIONS

The HgTe/CdTe SL single layers and SL-based HOT detector multilayer structures were grown using the MBE technique. The samples were characterized using FTIR, x-ray, and Hall effect measurements. The experimental results showed that we have good control over the material crystal quality. The FWHM values obtained through x-ray DCRCs were 100–150 arcsec, comparable with those of HgCdTe alloys grown on similar CdTe/Si substrates. Mesa-structure HOT devices were designed and successfully fabricated. The ex-situ gold doping technique was used for the p-type doping of the top layer of the structures. Spectral-response measurements demonstrate that the devices can give strong response at both 80 K and room temperature under zero bias conditions. The absorption coefficient calculated for an alloy with x = 0.38 showed good agreement with experiment at room

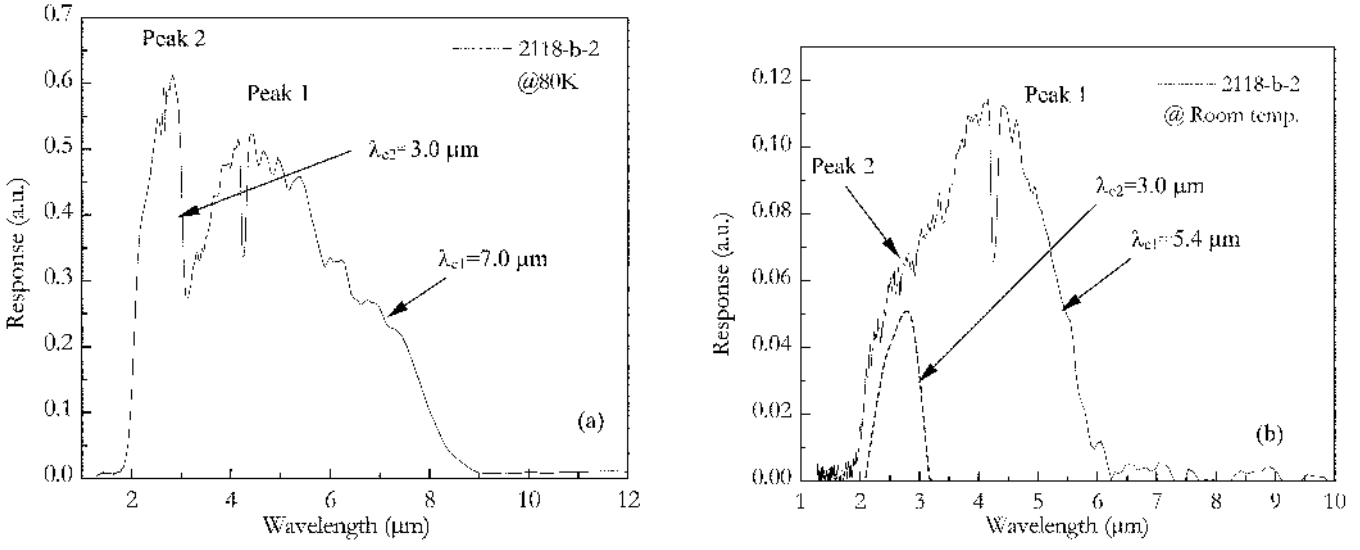

Fig. 8. Representative spectral-response curves for a device structured from sample hct2118 at (a) 80 K and (b) room temperature.

temperature. From the theoretical absorption coefficient for 80 K, the absorption edge of the alloy only shifts from 2.9 μm to 3.05 μm, whereas the absorption edge caused by the SL shifts from about 5 μm to 7 μm, which was in very good agreement with the spectral-response measurements.

With such unoptimized junctions, we measured detectivities that are very encouraging for these types of devices. Nevertheless, the encouraging results obtained in this study must stimulate further interest to revisit HgTe/CdTe-based SLs for advanced applications demanding very long wavelength response and HOT detectors. We can conclude from these preliminary results that the HgTe/CdTe SL systems have the potential to emulate industry-standard, HgCdTe-alloy systems.

ACKNOWLEDGEMENT

This work was supported by NASA under Grant No. NAG5-10334.

REFERENCES

1. J.N. Schulman and T.C. McGill, *Appl. Phys. Lett.* 34, 663 (1979).
2. C.R. Becker, V. Latussek, A. Pfeuffer-Jeschke, G. Landwehr, and L.W. Molenkamp, *Phys. Rev. B* 62, 10353 (2000).
3. Y.D. Zhou, C. Becker, Y. Selamet, Y. Chang, R. Ashokan, R.T. Boreiko, T. Aoki, D. Smith, A. Betz, and S. Sivananthan, *J. Electron. Mater.* 32, 608 (2003).
4. Y. Selamet, A. Ciani, C.H. Grein, and S. Sivananthan, *Proc. SPIE* 4795, 8 (2002).
5. G.L. Hansen and J.L. Schmit, *J. Appl. Phys.* 53, 1639 (1983).
6. J.D. Vincent, *Fundamentals of Infrared Detector Operation and Testing* (New York: John Wiley and Sons, 1989), p. 64.